Vol. 57: 1–18, 2009
doi: 10.3354/ame01317

AQUATIC MICROBIAL ECOLOGY
Aquat Microb Ecol

Printed October 2009
Published online September 9, 2009

Comparison of free-living, suspended particle, and aggregate-associated bacterial and archaeal communities in the Laptev Sea

Colleen T. E. Kellogg*, Jody W. Deming

School of Oceanography, University of Washington, Box 357940, Seattle, Washington 98195, USA

ABSTRACT: In cold oceans, the importance of microbes in degrading particulate organic matter (POM) and constraining carbon export has been questioned, given that a greater proportion of primary production reaches the seafloor at high latitudes than low latitudes. To learn more about POM-associated microbial communities in cold waters, we worked aboard the icebreaker 'Kapitan Dranitsyn' during the Nansen and Amundsen Basins Observational System (NABOS) 2005 cruise to the Laptev Sea, a river-impacted region in the Siberian Arctic, to sample 3 size fractions of particles operationally defined as sinking aggregates (>60 µm), smaller suspended particles (1 to 60 µm), and free-living bacteria (0.22 to 1 µm). Sample temperatures and depths ranged from –1.6 to 1.5°C and 25 to 150 m, respectively. Analysis of associated microbial communities using 16S rRNA gene-based clone libraries and terminal restriction fragment length polymorphism (T-RFLP) indicated greatest diversity and richness in the smaller size fractions and significantly different communities in the aggregate fraction for both Bacteria and Archaea. The most abundant clones in the bacterial libraries were *Gammaproteobacteria*, followed by members of the *Cytophaga-Flavobacterium-Bacteroides* (CFB) group and *Alphaproteobacteria*; the archaeal libraries contained primarily Marine Group I Crenarchaeota. Canonical correspondence analysis indicated that bacterial communities, especially those associated with aggregates, were influenced by riverine input and temperature. Determinants of archaeal communities were less clear, but temperature appeared important. Distinctions in bacterial and archaeal community complexity observed among the different particle size classes suggest the importance of particle residence time in structuring associated microbial communities and defining their biogeochemical roles.

KEY WORDS: Particle flux · Particle-associated microbes · T-RFLP · Lena River · Arctic Ocean

INTRODUCTION

In the Arctic Ocean, a large proportion (up to 50%, Buesseler 1998) of sinking particulate organic matter (POM) escapes pelagic recycling to reach the seafloor, especially on Arctic shelves (e.g. Cochran et al. 1995) where the material can support a productive benthic community. Arctic shelves, which comprise 35% of the total area of the Arctic Ocean, are important sites of POM transformation and advection to the deep Arctic Basin (Carroll & Carroll 2003, Bates et al. 2005, Forest et al. 2007). They are also heavily influenced by riverine input: the Arctic Ocean contains only 1% of global ocean water yet receives nearly 10% of global river discharge. Climate warming brings the potential for altered cycling and export of POM on Arctic shelves through permanent reductions in ice cover, increases in riverine discharge (Holland et al. 2007, Serreze et al. 2007), and incursions of warm Atlantic water, as in the Laptev Sea (Dmitrenko et al. 2008). Characterizing present carbon cycling and microbial participants on Arctic shelves in seasonally ice-free waters or polynyas is needed to help understand how the fate of organic matter may change as the Arctic continues to warm (Forest et al. 2007).

*Email: ctebean@u.washington.edu

Elsewhere in the global ocean, bacteria play significant roles in the attenuation of POM fluxes (Cho & Azam 1988, Karner & Herndl 1992, Simon et al. 2002). They are also known to develop distinctive communities on macroaggregates or marine snow, retrieved from surface waters and believed to be important to vertical carbon flux (DeLong et al. 1993, Rath et al. 1998, Simon et al. 2002), and on smaller particles that remain suspended longer (Crump et al. 1999, Fandino et al. 2001, Selje & Simon 2003, Johnson et al. 2006). Few studies have addressed the influence of bacteria on particle fluxes in the Arctic (Huston & Deming 2002) or the diversity of microbial communities associated with POM sinking through the 'twilight' zone of any ocean.

Pelagic microbial diversity in the Arctic has been studied based on whole water samples collected from the central Arctic (Bano & Hollibaugh 2002), Chukchi Sea (Hodges et al. 2005, Kirchman et al. 2007), and the river-impacted Mackenzie Shelf of the eastern Beaufort Sea (Wells & Deming 2003, Galand et al. 2006, Garneau et al. 2006, Wells et al. 2006). Inshore-offshore gradients in the diversity of pelagic Bacteria have been observed by fluorescence *in situ* hybridization (FISH), with *Betaproteobacteria* dominating inshore, *Alphaproteobacteria* dominating offshore, and *Cytophaga-Flavobacterium-Bacteroides* (CFB) and *Gammaproteobacteria* increasing in importance offshore (Garneau et al. 2006). Archaeal communities have also been deduced to shift geographically, with Archaea of apparent terrestrial origin detected in nearshore turbid waters, and marine forms dominating offshore (Galand et al. 2006, Garneau et al. 2006). Neither archaeal nor bacterial diversity has been reported for deeper waters on this or any Arctic shelf, or for aggregates descending into them, but elevated percentages of Archaea have been observed by FISH in nepheloid layers (particle-rich waters) advecting offshore at depth (Wells & Deming 2003, Wells et al. 2006).

In the one Arctic study that has attempted to distinguish particle-associated from free-living microbial diversity, the comparison was between whole water and the <3 µm sized fraction during the course of a bloom in the Chukchi Sea (Hodges et al. 2005). The 2 communities diverged most from each other when the bloom index (POM, total organic carbon [TOC], and chlorophyll *a* [chl *a*] concentrations) was high. This result and a corresponding drop in community richness are consistent with the concept that fresh marine organic matter exerts a selective force on associated microbial diversity (Simon et al. 2002). On a river-impacted shelf, where terrestrially derived aggregates of aged organic matter and associated microbes discharge into the ocean, mix with marine phytodetritus, sink to the seafloor, and resuspend in nepheloid layers, determining the forces at play on particle-associated microbial diversity becomes more challenging.

In other oceans, particle-associated bacteria are usually defined operationally by a filtration step, using a single filter pore size of typically 1 or 3 µm, to separate them from free-living bacteria. Large aggregates (marine snow) have also been collected, for example in diver-held samplers (DeLong et al. 1993), to compare aggregate-associated microbial communities with their free-living counterparts. We are not aware of oceanic studies where multiple size classes of particles have been collected for comparative analyses of microbial community structure, with each other and with the free-living community (see Dang & Lovell 2002 for such work in freshwater systems). Given the different residence times and histories of smaller suspended particles versus sinking aggregates in the ocean (Lee et al. 2004), especially on river-impacted shelves (Crump et al. 1999), the associated microbial communities can be expected to differ from each other as well as from their free-living counterparts.

In the present study, we took advantage of a rare opportunity for access to the Laptev Sea of the Siberian Arctic, an important component in the overall Arctic System for its hydrography and Atlantic connections (Dmitrenko et al. 2008), riverine influence and sedimentology (Boetius & Damm 1998, Wegner et al. 2005), and contributions to ice-rafted materials Arctic-wide (Eicken et al. 1997). We sampled 3 size classes of particles in surface and deeper waters: large sinking aggregates (AGG, >60 µm), smaller suspended particles (SSP, 1 to 60 µm), and the free-living microbial community (FL, 0.22 to 1 µm). The distinction between AGG and SSP was based on previous reports that particles larger than about 50 µm dominate vertical mass flux (Amiel et al. 2002 and references therein, Lee et al. 2004). To evaluate microbial diversity and richness, we generated bacterial and archaeal clone libraries and community fingerprints using terminal restriction fragment length polymorphism (T-RFLP) based on the 16S rRNA gene. Measured environmental variables included temperature, salinity, and particle content of the sampled waters (concentrations of total suspended matter, particulate organic carbon [POC], particulate organic nitrogen [PON], chl *a*, phaeopigments, and bacteria). Our goals were to determine and compare bacterial and archaeal community structures among the 3 particle size fractions sampled and how regional environmental factors, including riverine input on this Arctic shelf, might help to explain microbial patterns.

MATERIALS AND METHODS

Sample locations and collection. Samples were collected at 11 stations along 3 north–south transects (western, central, and eastern) and a fourth along-shelf

transect in the Laptev Sea of the Siberian Arctic (Fig. 1) from the Russian icebreaker 'Kapitan Dranitsyn' during the Nansen and Amundsen Basins Observational System (NABOS) cruise of 3 to 27 September 2005. Seawater was collected in project-dedicated (no delay in sample recovery) 10 l Niskin bottles mounted on CTD rosette deployed at routine depths of 25 and 100 m. The latter depth varied according to station depth, which ranged from 90 to 3100 m (navigational restrictions precluded sampling further inshore). At 2 stations, only 25 m samples were collected, due to start-up procedures (Stn 1) or rosette failure (Stn 19). Large grazers were removed by 600 µm Nitex mesh as water was drained into 10 l sterile Cubitainers (Hedwin) and moved immediately to a cold room at 6°C (coldest temperature achievable). There, a full Cubitainer of seawater was size-fractionated for analyses of microbial community structure. Additional volumes of water were collected to measure concentrations of total suspended particulate matter (SPM), chl *a* and phaeopigments, POC and PON, and bacterial abundance. CTD data (temperature and salinity) were provided by I. Dmitrenko (GEOMAR, Kiel, Germany) and inorganic nutrient data (nitrate, phosphate, and silicate) by M. Nitishinsky (Arctic and Antarctic Research Institute, St. Petersburg, Russia).

Analysis of environmental factors. ***SPM:*** Duplicate 1 l water samples were vacuum-filtered through precombusted (5 h at 500°C), pre-weighed 1.2 µm GF/C filters (Whatman). Each filter was then rinsed with 10 ml of 1% sodium formate to dissolve salts, transferred to a sterile Petri dish, stored at –20°C, and kept frozen during transport to Seattle. Filters were dried at 60°C for 24 h and weighed again. SPM was calculated as the difference between final and initial weight.

POC and PON: Duplicate 350 to 400 ml water samples were vacuum-filtered through pre-combusted 25 mm GF/F filters (Whatman). Each filter was folded in half (sample side inwards), placed in a pre-combusted foil pouch and stored and transported frozen, as for SPM. Samples were later thawed, dried at 60°C, fumed with HCl vapor to remove the carbonate fraction, and dried again (overnight for each step). POC and PON were quantified using a Leeman Labs Model CEC440 Elemental Analyzer.

Chl a and phaeopigments: Duplicate 350 to 400 ml water samples were filtered through pre-combusted GF/F filters. Each filter was placed into a pre-combusted foil pouch and stored and transported frozen, as for SPM. Chl *a* and phaeopigment concentrations were measured using standard colorimetric analyses, according to Parsons et al. (1984).

Total bacterial abundance: Water volumes of 40 ml were placed in sterile, screw-cap 50 cm^3 tubes and fixed with pre-filtered (0.22 µm) 37% formaldehyde to final concentration of 2%. Samples were kept refrigerated until analyzed microscopically, using a Zeiss Universal epifluorescent microscope, within 2 mo of collection. Subsamples of 5 to 10 ml were gently filtered onto a 0.22 µm polycarbonate filter and stained with acridine orange and DAPI, according to the dual-staining technique of Schmidt et al. (1998) optimized for seawater (Collins et al. 2008). Twenty fields or a minimum of 200 cells were counted to calculate bacterial abundance; the average of duplicate subsamples is reported.

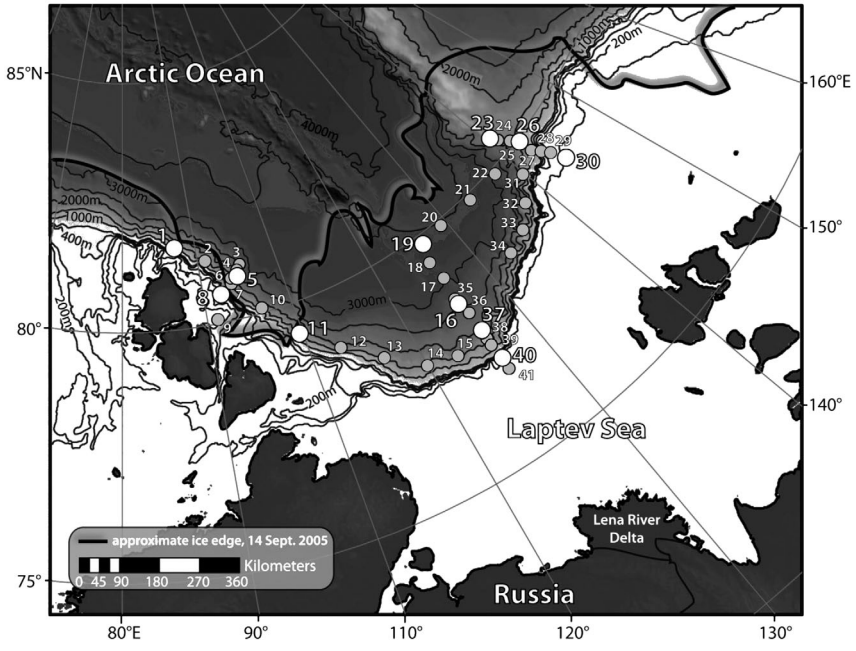

Fig. 1. Map of stations visited during the Nansen and Amundsen Basins Observational System (NABOS) expedition of 2005. Three north-south transects (Western, Central, and Eastern Laptev Sea) and 1 along-shelf transect were carried out during NABOS 2005. ○: stations sampled; ●: stations visited but not sampled

Analysis of microbial community structure. ***Sample processing:*** For DNA analyses, 7 to 10 l of water were gently filtered through an in-line filtration system consisting of a 60 µm nylon net filter (Millipore; to collect AGG), 1 µm polycarbonate filter (GE Osmonics; to collect SSP), and a 0.22 µm Sterivex™ GV filter (Millipore; to collect FL microbes). The 60 µm and 1 µm filters were placed into autoclaved 1.5 ml microcentrifuge tubes which then received 500 µl of extraction buffer (0.75 M sucrose, 40 mM EDTA, 50 mM Tris-HCl, pH 8.3) via 0.2 µm syringe

filter. About 1 ml of buffer was pushed through the Sterivex^{TM} filter before adding another 1.8 ml to the filter unit and capping it. All filters were frozen at –20°C, transported frozen to Seattle, then transferred to –80°C.

DNA extraction: The nucleic acid extraction protocol followed Massana et al. (1997) with some modifications. Extractions of FL (on Sterivex^{TM} filters) and SSP and AGG (on filters in microcentrifuge tubes) samples began with addition of lysozyme (1 mg ml^{-1}) and incubation at 37°C for 30 min. Proteinase K (0.5 mg ml^{-1}) and sodium dodecyl sulfate (SDS) (1%) were added, and filters were incubated at 55°C for 1 to 2 h. Lysate was recovered from the filters, with lysate from Sterivex^{TM} samples divided into four 500 µl aliquots. Lysates were extracted twice with phenol-chloroform-isoamyl alcohol (25:24:1; pH 8) and once with chloroform-isoamyl alcohol (24:1). RNA was degraded by adding RNase (2 µg ml^{-1}) and incubating at 37°C for 30 min. DNA was precipitated using standard ethanol precipitation (Van Mooy et al. 2004a). After samples were dry, extracted DNA was suspended in 100 µl TE (10 mM Tris-Cl, pH 7.5 1 mM EDTA), vortexed, and stored at –20°C. Samples initially subdivided were recombined after the initial ethanol precipitation, re-precipitated and resuspended in 100 µl TE.

PCR amplification of 16S rRNA gene: Archaeal and bacterial 16S rRNA genes were amplified in a reaction mixture containing 1 × $MgCl_2$-free Taq DNA Polymerase buffer (Promega), 2.0 mM $MgCl_2$, 200 µM each deoxyribonucleotide triphosphate, 0.01 µM forward primer (Table 1), 0.01 µM reverse primer (Table 1), 0.2 U Taq DNA Polymerase (Promega), 2 µl template DNA, and distilled and deionized water (dH_2O) to a final volume of 20 µl. For T-RFLP analyses, the 16S rRNA gene was amplified using fluorescently (FAM) labeled primers (Table 1). Samples were diluted 10- to 100-fold with T-low-E (1 M Tris-HCl, 0.5 M EDTA, pH: 8.0) prior to amplification to reduce inhibitors. The general program for amplification was 1 cycle of a 4 min denaturing step at 94°C; 30 cycles of 1 min denaturing at 94°C, 1 min annealing at temperature appropriate for primer pairs used (Table 1), and 2 min of extension at 72°C; and a final extension for 10 min at 72°C followed by at least 10 min at 4°C. The products of 3 to 6 reactions were pooled to obtain sufficient concentrations of DNA, cleaned using a Qiaquick PCR purification kit, and resuspended in 30 µl of Buffer EB supplied with the Qiaquick kit.

Clone library construction: Three bacterial clone libraries were generated from surface waters of Stn 8, 1 from each of the 3 size fractions, using the 16S rRNA gene amplified with the 27f/1492r primer pair (Table 1). Two archaeal clone libraries were generated from the surface waters of Stn 26, 1 each from the FL and SSP size fractions, using the 16S rRNA gene amplified with the 21f/958r primer pair (Table 1). We tried to develop archaeal clone libraries from Stn 8 and the AGG sample at Stn 26, but the extracted DNA did not amplify (as it did with T-RFLP primers). PCR products were topoisomerized into pCR4-TOPO vectors (Invitrogen) and used to transform One Shot TOP10 chemically competent *Escherichia coli* cells (Invitrogen). All cloning followed the manufacturer's instructions.

Sequencing: Most samples were sequenced at the High-Throughput Genomics Unit (HTGU) at the University of Washington (UW), using an ABI 3730xl (Applied Biosystems) capillary sequencer. Between 40

Table 1. Names and sequences of PCR primers used. *E. coli*: *Escherichia coli*; temp.: temperature; T-RFLP: terminal restriction fragment length polymorphism; sequencing: primers were used in the initial amplification of the 16S rRNA gene, prior to cloning; vector: the primers target the vector (TOPO4-TA) for cloning

Target domain	Use	Sequence	Annealing temp. (°C)	5′ *E. coli* start	3′ *E. coli* end	Source
Bacteria	T-RFLP/sequencing	AGA GTT TGA TCM TGG CTC AG	55	8	27	Lane (1991)
Bacteria	T-RFLP/sequencing	GGY TAC CTT GTT ACG ACT T	55	1510	1492	Lane (1991)
Bacteria	Cycle sequencing	CAG CMG CCG CGG GTA ATW C	50[a]	519	536	Suzuki & Giovannoni (1996)
Bacteria	Cycle sequencing	GWA TTA CCG CGG CKG CTG	50[a]	536	519	Amann et al. (1995)
Bacteria	Cycle sequencing	AAA CTY AAA GGA ATT GAC GG	50[a]	907	926	Crump et al. (2003)
Bacteria	Cycle sequencing	CCG TCA ATT CCT TTR AGT TT	50[a]	926	907	Crump et al. (2003)
Archaea	Sequencing	TTC CGG TTG ATC CYG CCG GA	59	2	21	DeLong (1992)
Archaea	Sequencing	YCC GGC GTT GAM TCC ATT	59	976	958	DeLong (1992)
Archaea	T-RFLP	ACK GCT CAG TAA CAC GT	57	109	125	Großkopf et al. (1998)
Archaea	T-RFLP	GTG CTC CCC CGC CAA TTC CT	57	934	915	Großkopf et al. (1998)
Archaea	Cycle sequencing	GTG CCA GCM GCC GCG GTA	50[a]	515	533	Moyer et al. (1998)
Archaea	Cycle sequencing	TTA CCG CGG CKG CTG GCA C	50[a]	533	515	Moyer et al. (1998)
Vector	Cycle sequencing	GTA AAA CGA CGG CCA G	50[a]	370	355	Invitrogen
Vector	Cycle sequencing	CAG GAA ACA GCT ATG AC	50[a]	205	221	Invitrogen

[a]50°C was the suggested annealing temperature for the cycle sequencing reaction used

and 105 clones were chosen randomly from each clone library and screened for the presence of an insert. Fewer clones were screened for archaeal sequencing due to observed low apparent natural diversity; more clones were sequenced for bacterial libraries due to presence of chloroplast sequences. Transformed clones were sequenced with multiple primers (Table 1) to obtain bi-directional, double-stranded sequences.

Some sequencing was done at the UW Marine Molecular Biotechnology Lab (MMBL) where clone libraries were subjected to dye-termination sequencing using 4 µl MegaBACE Premix (Amersham Biosciences), 0.1 µM primer (Table 1), 2 µl plasmid DNA, and dH_2O to 10 µl, and the following thermocycling conditions: 40 cycles of 94°C for 15 s, 50°C for 20 s, and 60°C for 2 min. Sequencing reactions were precipitated with 27.5 µl absolute ethanol and 1 µl 7.5 M ammonium acetate, centrifuged for 30 min at 3100 × g, decanted, washed with 200 µl 70% ethanol, centrifuged for 15 min at 3100 × *g*, and air-dried. Samples were resuspended in 5 µl of formamide loading solution and sequencing reactions were run on a MegaBACE1000 capillary electrophoresis sequencer. As at HTGU, clones at MMBL were also sequenced bi-directionally.

Phylogenetic analyses: Forward and reverse sequences were assembled and edited using the program Sequencer 4.6 (Gene Codes). Sequences were checked for chimeras using the Bellepheron tool supplied as part of the Greengenes database (http://greengenes.lbl.gov; DeSantis et al. 2006) and cross-checked using the Mallard program (www.bioinformatics-toolkit.org/Mallard/index.html; Ashelford et al. 2006). No chimeric sequences were detected in the archaeal clone libraries or the AGG bacterial clone library; those detected in the SSP bacterial library (3) and FL bacterial library (8) were removed. Reference sequences closely related to obtained sequences were acquired using BLAST (http://blast.ncbi.nlm.nih.gov/Blast.cgi). Edited sequences were aligned automatically using ClustalX (http://bips.u-strasbg.fr/fr/Documentation/ClustalX/) and checked and trimmed for phylogenetic analyses to lengths of ~1060 bp for bacterial sequences (except for 2 sequences of 790 bp length) and of ~760 bp for archaeal sequences using Bioedit (Ibis Therapeutics). DNADIST from PHYLIP (v. 3.66; http://evolution.genetics.washington.edu/phylip.html) was used to calculate genetic distances by the Kimura-2 model, with 100 data sets obtained by bootstrapping using SEQBOOT. Phylogenetic trees were estimated using FITCH in PHYLIP. Bootstrap values obtained from a consensus bootstrap tree, also created using FITCH and CONSENSE, were hand-mapped onto a distance tree. One tree was created for the 3 bacterial clone libraries and 1 for the 2 archaeal libraries.

The number of phylotypes in each library and the diversity indices (Chao1 for library richness, and Shannon-Wiener index for library diversity) were estimated using the program DOTUR (Schloss & Handelsman 2005). Phylotypes were defined as sequences of ≥ 97% similarity (for SSP and FL bacterial clone libraries) or ≥ 99% similarity when DOTUR did not provide the 97% option (remaining libraries) due to low diversity or low number of sequences. Library percent coverage was estimated using the method of Good: $(1 - [n/N]) \times 100$, where n represents the number of unique clones and N, the sample size (Galand et al. 2003).

Nucleotide sequence accession numbers: The 16S rRNA gene sequences were submitted to the GenBank database (www.ncbi.nlm.nih.gov/Genbank/) and given the accession numbers EU544675 through EU544862.

T-RFLP: For each sample amplified with fluorescently labeled (FAM) primer (Table 1), cleaned PCR product was used to generate a microbial fingerprint and estimate richness, according to the T-RFLP technique of Moeseneder et al. (1999) as modified by Van Mooy et al. (2004b). A 2 to 4 µl volume of cleaned, labeled PCR product (~50 ng DNA across the study) was added to a cocktail of 1 µl of buffer provided with the restriction enzyme (RE), 2 units of the desired RE, and dH_2O to bring the reaction volume to 10 µl. We used four 4-cutter REs (Fermentas): *Bsu*RI (5′-G G^CC-3′), *Hha*I (5′-GCG^C-3′), *Rsa*I (5′-GT^AC-3′), or *Msp*I (5′-C^CGG-3′). Bacterial DNA was digested with *Bsu*RI, *Hha*I, or *Rsa*I; and archaeal DNA with *Bsu*RI, *Hha*I, or *Msp*I. Digestions were run for 6 h at 37°C and terminated using heat shock (at manufacturer-recommended temperatures) for 20 min. Restriction digests were purified by ethanol precipitation and stored dried at −20°C until analyzed. Samples were resuspended in a cocktail of dH_20, Tween-20, and MegaBACE ET900-R size standard (GE Biosciences) prior to identifying terminal restriction fragments on a 96-well MegaBACE Sequencer in genotyping mode at MMBL.

Results in the form of T-RFLP electropherograms were analyzed using the data acquisition program DAx (Van Mierlo Software Consultancy). Samples were scored for presence or absence of significant peaks at each bp length between 60 and 900 base pair (bp). Peak-calling criteria were adjusted for each RE due to differences in noise and peak clarity (Table 2). Fragment lengths were binned into 3 bp increments. Binned results were translated into binary format using the program Daxter (written by R. E. Collins: http://rocaplab.ocean.washington.edu/cgi/dakster/index.html) to represent the presence and absence of each of the 280 possible peaks. For comparative analysis, the lengths of terminal fragments from all clone library sequences were estimated after *in silico* digestion with the 3 T-RFLP enzymes, using the program Restriction Enzyme Picker (Collins & Rocap 2007).

Table 2. Criteria for determining significant operational taxonomic unit (OTU) using the program DAx (Van Mierlo Software Consultancy)

Domain	Enzyme	Minimum peak area	Signal: noise ratio	Slope
Bacteria	*Bsu*RI	0.1	25	0.06
	*Hha*I	0.06	20	0.03
	*Rsa*I	0.07	20	0.05
Archaea	*Bsu*RI	0.2	25	0.07
	*Hha*I	0.3	35	0.06
	*Msp*I	0.1	30	0.06

Data and statistical analyses. SPSS for Windows (v. 14.0) was used to conduct Pearson correlation analyses of the environmental variables and partial correlation analyses controlling for depth. One-way ANOVAs in Microsoft Excel were verified with SPSS. The program PAST (v. 1.79, Hammer et al. 2008) was used for principal component analysis (PCA) of the environmental variables, first normalizing each data point to the average of the variable: temperature, salinity, and concentrations of silicate, nitrate, phosphate, SPM, POC, PON, chl *a*, and phaeopigment, and total bacterial abundance.

T-RFLP electropherograms were analyzed using Primer 6 software (Primer-E). Similarity matrices created from presence/absence data were calculated between every pair of samples using the similarity coefficients of the Jaccard index. These matrices were used for non-metric multidimensional scaling (NMDS) plots and cluster analyses, which aid in visualizing the similarity between microbial communities by proximity in 2D space. An analysis of similarity (ANOSIM) was also used to test for the influence of particle size fraction on variation in community similarity data. ANOSIM combines permutation tests with basic Monte Carlo randomizations to examine predefined groups of samples for differences in community structure.

To combine the primary data sets and assess whether 1 or more environmental factors might explain some of the observed variability in community structure, we used the Multivariate Statistics Package (MVSP; Kovach Computing Services) for canonical correspondence analysis (CCA). In this gradient analysis, ordination of the T-RFLP data by particle size fraction and sample location was constrained by the measured environmental variables.

RESULTS

Field conditions

During the time of sampling, sea ice conditions in the Laptev Sea reflected the continuing downward trend in the areal extent of Arctic sea ice (http://nsidc.org/). The ice edge had retreated to the north and was not encountered for most of the expedition (Fig. 1). Mean air temperature was 0°C, except during 13 to 17 September, when it averaged −2°C. Skies were overcast for most of the sampling period.

In general, the CTD data indicated that the upper water column in the western regions of the study area was cold (average temperature −1.56 ± 0.13°C at 25 m) and salty (average salinity 33.4 ± 0.5 at 25 m; see Table A1, Appendix 1 for station-specific data). The eastern region was warmer (average temperature −0.75 ± 0.69°C at 25 m) and fresher (average salinity 30.6 ± 1.75), with the fresher surface layer extending deeper in the water column eastward, indicating the influence of Lena River outflow. The range in temperatures for the surface waters was narrow (−1.6 to −1.1°C). Only at western stations for our deepest samples (150 m), near the even deeper layer of warm Atlantic Water spreading along the Siberian continental margin (Dmitrenko et al. 2008), were above-zero water temperatures (1.3 and 1.5°C) encountered. Surface-water salinities indicated station groupings according to saltier waters (salinities of 32.0 to 34.1) in the western and alongshore central regions (Stns 1 to 11, 37, and 40) and fresher waters (salinities 28.6 to 30.8) in the eastern and offshore central regions (Stns 16 to 30). Deeper samples were salty throughout the region (salinities 33.7 to 34.8).

The range in SPM across all samples was also narrow (5.9 to 7.7 mg l^{-1}) with no relation to depth (1-way ANOVA). Chl *a* and phaeopigment concentrations were comparable in amount, low region-wide (0.01 to 0.68 and 0.01 to 0.53 µg l^{-1}, respectively) and also unrelated to depth. POC, however, was significantly ($p = 0.0099$) higher in surface waters (25.3 to 95.5 µg l^{-1}) than deeper waters (10.3 to 43.7 µg l^{-1}), as were PON ($p = 0.0034$) and total bacterial abundance ($p << 0.001$; 1.81×10^5 to 8.19×10^5 cells ml^{-1} in surface waters; 1.33×10^5 to 3.75×10^5 cells ml^{-1} in deeper waters; see Table A1, Appendix 1 for station-specific data).

Pearson correlation coefficients and partial correlation analysis confirmed that depth was a highly significant ($p < 0.001$) determinant of temperature, salinity, POC, PON, and bacterial abundance (as well as nitrate and phosphate). These analyses also supported the use of silicate as a riverine proxy, given the significant negative correlation of silicate with salinity ($r = -0.560$, $p < 0.05$), which strengthened when depth was controlled ($r = -0.749$). Our PCA analysis (Fig. A1, Appendix 2) revealed that surface samples from the more marine stations were associated with particulate variables, while fresher waters were associated with silicate.

Microbial community structure

Bacteria

The bacterial clone libraries created from FL, SSP, and AGG size fractions contained 42, 45, and 17 sequenced clones, respectively (Fig. 2). Additional clones were sequenced for the SSP and AGG libraries, but they proved to be eukaryotic chloroplast sequences (39% of SSP clones, 35% of AGG clones; none were detected in the FL library). Each of the bacterial libraries was dominated by *Gammaproteobacteria*, increasing in percentage as particle size fraction increased, from 71% (FL) to 78% (SSP) and 89% (AGG). Most of the FL clones clustered in 1 group, while many of the SSP and AGG clones clustered in another. Each library also contained representative clones from CFB at 14% (FL), 21% (SSP), and 6% (AGG). Only the FL and SSP libraries contained *Aphaproteobacteria*; only the AGG library contained *Gammaproteobacteria* (a single clone).

Coverage of the natural bacterial assemblages by these libraries was higher in the larger size fractions (71% for AGG and SSP versus 60% for FL), while the number of unique clones or phylotypes was higher for the smaller size fractions (17 and 13 in FL and SPP libraries versus 5 in the AGG library; Table 3). According to the Shannon-Wiener index of diversity and Chao1 estimate of richness, both diversity and richness were lowest in the AGG library and highest in the FL library (Table 3) in spite of the more limited coverage of the FL Bacteria.

Many of the samples collected for T-RFLP analysis proved difficult to amplify with bacterial primers, possibly due to the primer set chosen or the presence of humic substances. For the 19 samples amplified, bacterial richness, as estimated by the number of significant operational taxonomic units (OTUs) in the *Bsu*RI digests, was generally higher in both the FL and SSP size fractions than in the AGG samples. Although this comparative result held true for all enzymes used for T-RFLP, the *Bsu*RI digest results were used in NMDS and CCA analyses because they yielded electropherograms with slightly less noise. Of the observed T-RFLP OTUs (across all enzymes used), about one-third were identifiable using peaks predicted from the bacterial clone libraries (observed were within ±2 bp of predicted), likely due to libraries undersampling natural diversity. On the other hand, not all of the diversity present in the clone libraries was detected by T-RFLP; *in silico* digests of some of the sequenced clones from the libraries resulted in terminal fragments outside the detection limit of the electropherograms (<60 bp or >900 bp). Sequences identifiable as chloroplasts in T-RFLP electropherograms were few in number (0 to 2, with most samples containing 0 to 1) and frequently outside of the peak-calling range.

When NMDS was applied to the observed T-RFLP OTUs, AGG Bacteria emerged as communities distinctive from SSP or FL communities (Fig. 3). SSP and FL communities could not be distinguished from each other at the 20% similarity level, though a group separation appears within that cluster (Fig. 3). The dendrogram resulting from cluster analysis (not shown) indicated that these communities from the smaller size fractions were at least 50% similar.

The results of an ANOSIM test allowed rejection of the null hypothesis that bacterial communities in each size fraction are the same. ANOSIM gives an R statistic (which ranges between 0 and 1) in addition to a p-value, where the higher R is, the greater the difference in community structure. For bacterial T-RFLP results, significant ($p < 0.01$) differences were observed between AGG communities and the 2 smaller size fractions for all 3 restriction enzymes used (Table 4). The R statistic for FL versus AGG was always higher (0.756 to 0.929) than for SSP versus AGG (0.506 to 0.630). Comparative tests between FL and SSP communities indicated no significant difference by *Bsu*RI and significant ($p < 0.05$) differences by *Hha*I and *Rsa*I, but low R statistics (0.187 to 0.346) for all 3 enzymes (Table 4). Comparing the observed richness between size fractions by ANOVA gave similar results to the ANOSIM tests: no significant difference ($p > 0.05$) between FL and SSP samples, but significant differences ($p < 0.05$) between pairwise comparisons of AGG with both FL and SSP (Table 4).

Archaea

The clone libraries created for FL and SSP consisted of 38 and 46 clones, respectively (Table 3). Each library revealed low archaeal diversity, dominated by Marine Group (MG) I Crenarchaeota (97% and 98%, respectively), all of which were >97% similar in 16S rRNA gene sequence (Fig. 4). Each library also contained 1 clone representing a MG II Euryarchaeote. The estimated coverage was 95% for the FL library and 96% for the SSP library (Table 3). At the 1% sequence distance level, both libraries contained only 2 unique clones (Table 3). According to the Shannon-Wiener index of diversity, the FL library was only slightly more diverse than the SSP library; both were much less diverse than their bacterial counterparts. The Chao1 richness estimate for both libraries was only 2 (Table 3).

Archaeal 16S rRNA genes were more amenable to amplification for T-RFLP analyses than bacterial 16S rRNA genes, resulting in 44 amplified samples,

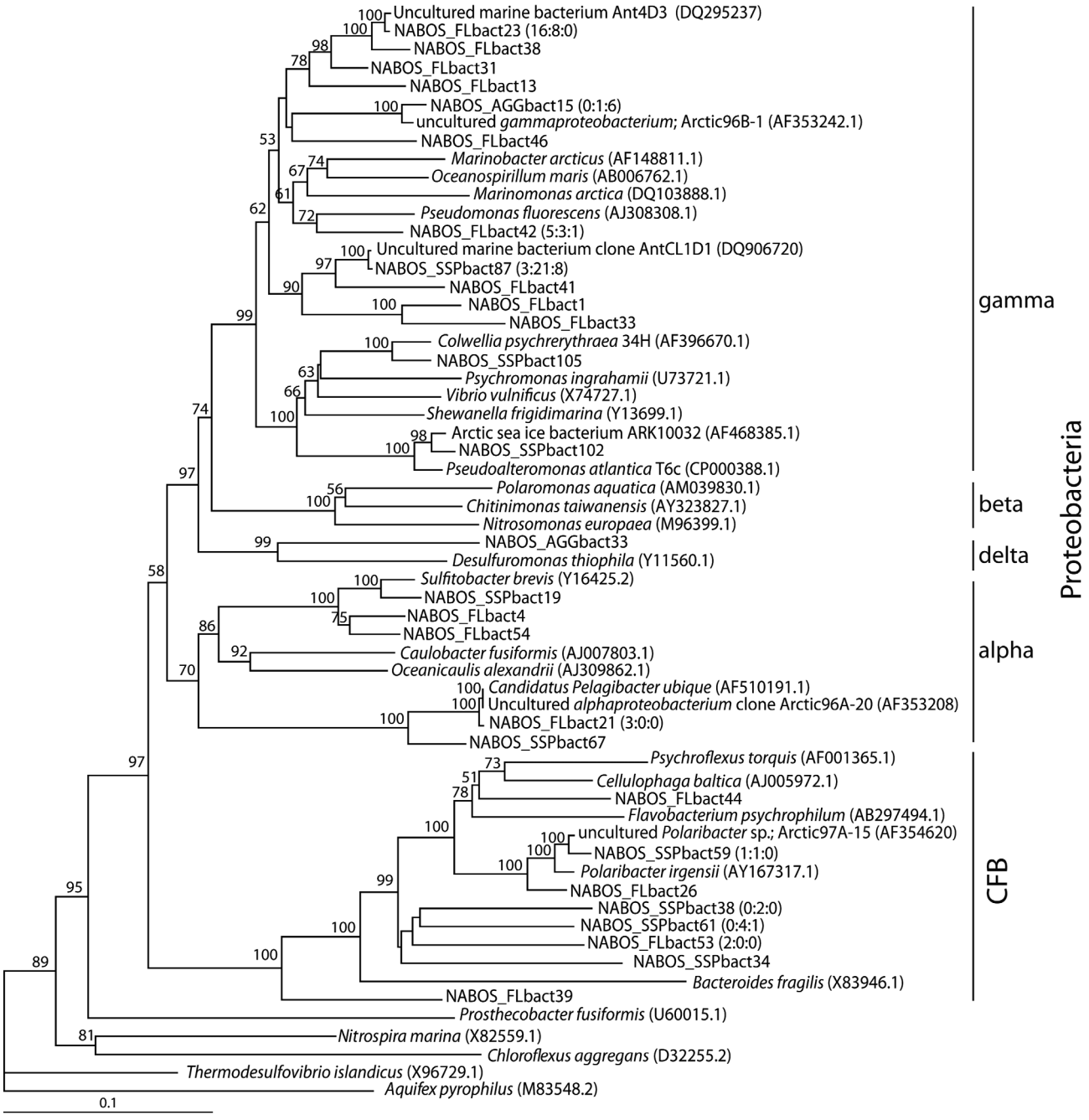

Fig. 2. Phylogenetic tree of all sequenced clones from bacterial 16S rRNA gene-based clone libraries of the free-living (FL), small suspended particle (SSP), and aggregate (AGG) size fractions of surface water at Stn 8. Clones are denoted NABOS_FLbactX, NABOS_SSPbactX, or NABOS_AGGbactX where X is the clone number. Numbers in parentheses indicate number of clones from each size fraction (FL:SSP:AGG) that are >97% similar to the given clone. This distance tree was created using the FITCH tool included in PHYLIP v. 3.66. The reference bar represents 0.1 substitutions per nucleotide site. Bootstrap values were mapped onto this tree from a consensus bootstrap FITCH tree created from 100 replicates. *Aquifex pyrophilus* was used as an outgroup. gamma: *Gammaproteobacteria*; alpha: *Alphaproteobacteria*; delta: *Deltaproteobacteria*; beta: *Betaproteobacteria*; CFB: *Cytophaga-Flavobacterium-Bacteroides* group

including more AGG samples. Although the cloning results suggested that we had sampled natural archaeal diversity well by that method, the T-RFLP results revealed greater richness (22 OTUs in some samples digested with *Bsu*RI). Richness was lower than observed for Bacteria (mean of 13 versus 28 OTUs per sample), but trends among the different size fractions were similar: observed archaeal rich-

Table 3. Diversity calculations for the bacterial and archaeal clone libraries from surface waters. Diversity estimators were calculated at a 3% distance level for free-living (FL) and small suspended particle (SSP) Bacteria and 1% for aggregate (AGG) Bacteria and all Archaea. Chao1: an estimate of richness; *H′*: Shannon-Wiener index of diversity

Domain	Stn	Size fraction	No. of clones	No. of phylotypes	% Coverage	*H′*	Chao1
Bacteria	8	FL	42	17	59.5	2.27	35
	8	SSP	45	13	71.1	1.88	27
	8	AGG	17	5	70.6	1.22	8
Archaea	26	FL	38	2	94.7	0.123	2
	26	SSP	46	2	95.6	0.105	2

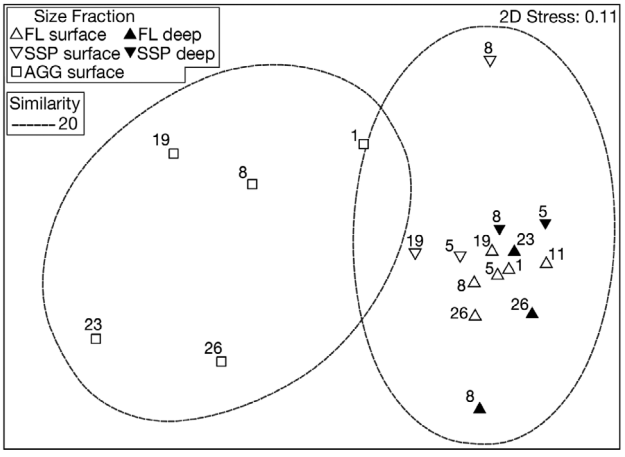

Fig. 3. Non-metric multidimensional scaling (NMDS) plot for bacterial terminal restriction fragment length polymorphism (T-RFLP) results. Samples within the dashed circles are 20% similar in community structure. Aggregate (AGG) samples group together (left circle) and separately from the smaller size fractions (free living [FL] and small suspended particles [SSP]). AGG samples from deeper waters are absent due to recalcitrance to amplification

ness was generally greater in the smaller size fractions than in the AGG samples. As for the Bacteria, results from the *Bsu*RI digests were used for archaeal NMDS and CCA analyses.

Of the observed archaeal T-RFLP OTUs, 26% were identifiable on average using the peaks predicted from *in silico* digests of Archaea in the clone libraries. The same criteria for an identifiable OTU (±2 bp) were used for both Archaea and Bacteria, but the ability to identify archaeal peaks in a given electropherogram varied more, in keeping with the discrepancy in richness observed between archaeal clone libraries and T-RFLPs (likely attributable to use of different primer pairs). For example, some samples contained 100% of the OTUs predicted by *Hha*I digests, while others contained none of them. Nevertheless, most T-RFLP samples contained the cloned OTU representative of the MG I Crenarchaeote, which dominated both archaeal libraries, as well as the MG II Euryarchaeote OTU.

NMDS analysis of archaeal T-RFLP OTUs indicated a distinction between communities by size fraction, as did cluster analysis (results not shown), with AGG samples grouping separately from FL and SSP communities (Fig. 5). The separation was not as exclusive as for Bacteria: more overlap occurred between samples of different size fractions in 2D space. Although FL and SSP archaeal communities, like their bacterial counterparts, could not be distinguished from each other at the 20% similarity level by NMDS, observed FL archaeal richness differed significantly from both SSP and AGG

Table 4. Comparison of richness (ANOVA) and diversity (analysis of similarities, ANOSIM) of Bacteria and Archaea (by terminal restriction fragment length polymorphism, T-RFLP) between different size fractions of the samples collected, successfully amplified, and digested by different restriction enzymes. Single-factor ANOVA results ($\alpha = 0.05$): ns denotes no significant difference in observed richness between size fractions and + denotes a significant difference. ANOSIM results: if R = 0, the community structures are identical while if R = 1, they have no similarity; $p < 0.05$ indicates that R is significant while $p < 0.01$ indicates that R is highly significant. AGG: aggregate; FL: free living; SSP: small suspended particles

Domain	Enzyme	FL vs. SSP			SSP vs. AGG			FL vs. AGG		
		ANOVA	R	p	ANOVA	R	p	ANOVA	R	p
Bacteria	*Bsu*RI	ns	0.187	0.092	+	0.630	0.008	+	0.909	0.002
	*Hha*I	ns	0.346	0.017	+	0.506	0.008	+	0.756	0.002
	*Rsa*I	ns	0.266	0.035	+	0.528	0.008	+	0.929	0.002
Archaea	*Bsu*RI	+	0.116	0.012	+	0.351	0.001	+	0.794	0.001
	*Hha*I	ns	0.081	0.028	+	0.400	0.001	+	0.722	0.001
	*Msp*I	+	0.216	0.002	+	0.557	0.001	+	0.903	0.001

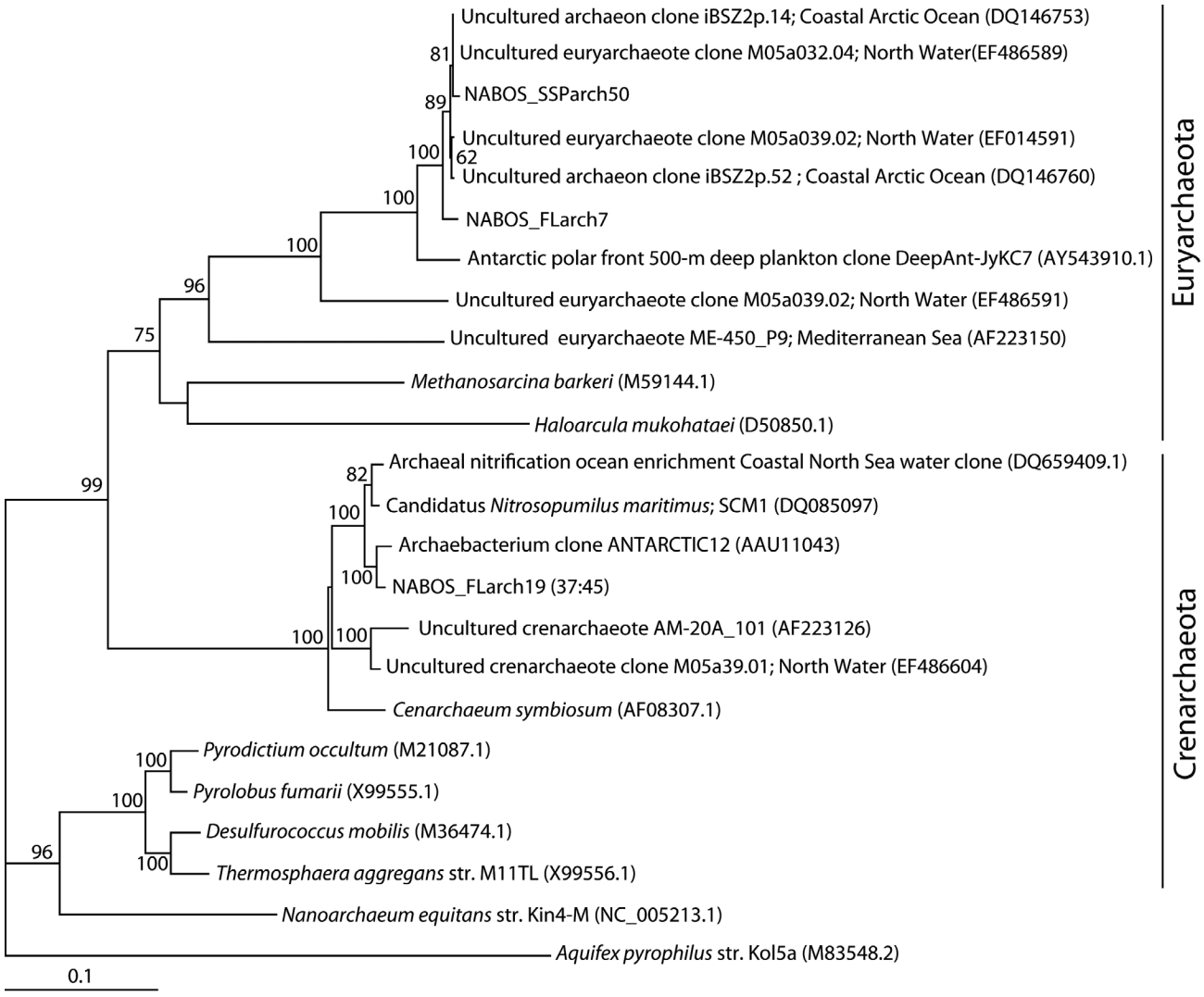

Fig. 4. Phylogenetic tree of all sequenced clones from archaeal 16S rRNA gene-based clone libraries of the free-living (FL) and small suspended particle (SSP) size fractions of surface water at Stn 26. Clones are denoted NABOS_FLarchX or NABOS_SSParchX where X is the clone number. Numbers in parentheses next to 1 clone (NABOS_FLarch19) indicate the number of clones from each size fraction (FL:SSP) that are 100% similar to the clone shown. This distance tree was created using the FITCH tool included in PHYLIP v. 3.66. The reference bar represents 0.1 substitutions per nucleotide site. Bootstrap values were mapped onto this tree from a consensus bootstrap FITCH tree created from 100 replicates. *Aquifex pyrophilus* was used as an outgroup

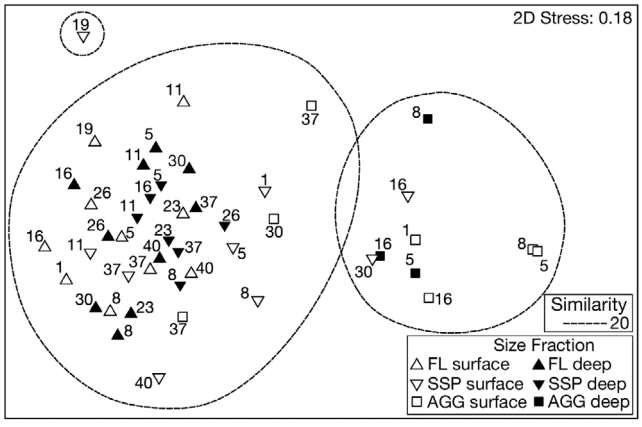

Fig. 5. Non-metric multidimensional scaling (NMDS) plot for archaeal terminal restriction fragment length polymorphism (T-RFLP) results. Samples within the dashed circles are 20% similar in community structure. Aggregate (AGG) samples group together (right circle) and separately from the smaller size fractions (free living [FL] and small suspended particles [SSP]), although some overlap exists between SSP and AGG samples (not observed for Bacteria, Fig. 3)

richness by ANOVA (for all 3 enzymes, Table 4). All pairwise comparisons by ANOSIM were significant, but FL and SSP comparisons (with lowest R statistics) indicated that these communities differed the least from each other. As for Bacteria, community comparisons between FL and AGG Archaea were highly sig-

nificant with the highest R statistics, the latter indicating that of the 3 pairwise comparisons, these communities differed the most from each other. Examining relationships between archaeal AGG diversity in surface and deeper water samples revealed that no surface sample plotted coincidentally in space with its deeper paired sample (Fig. 5).

Environmental control of microbial community structure

In the CCA comparing bacterial community structure and environmental factors (Fig. 6), most of the variation in community structure was explained by the first 3 axes (26, 16.9, and 14.6%) for which species-

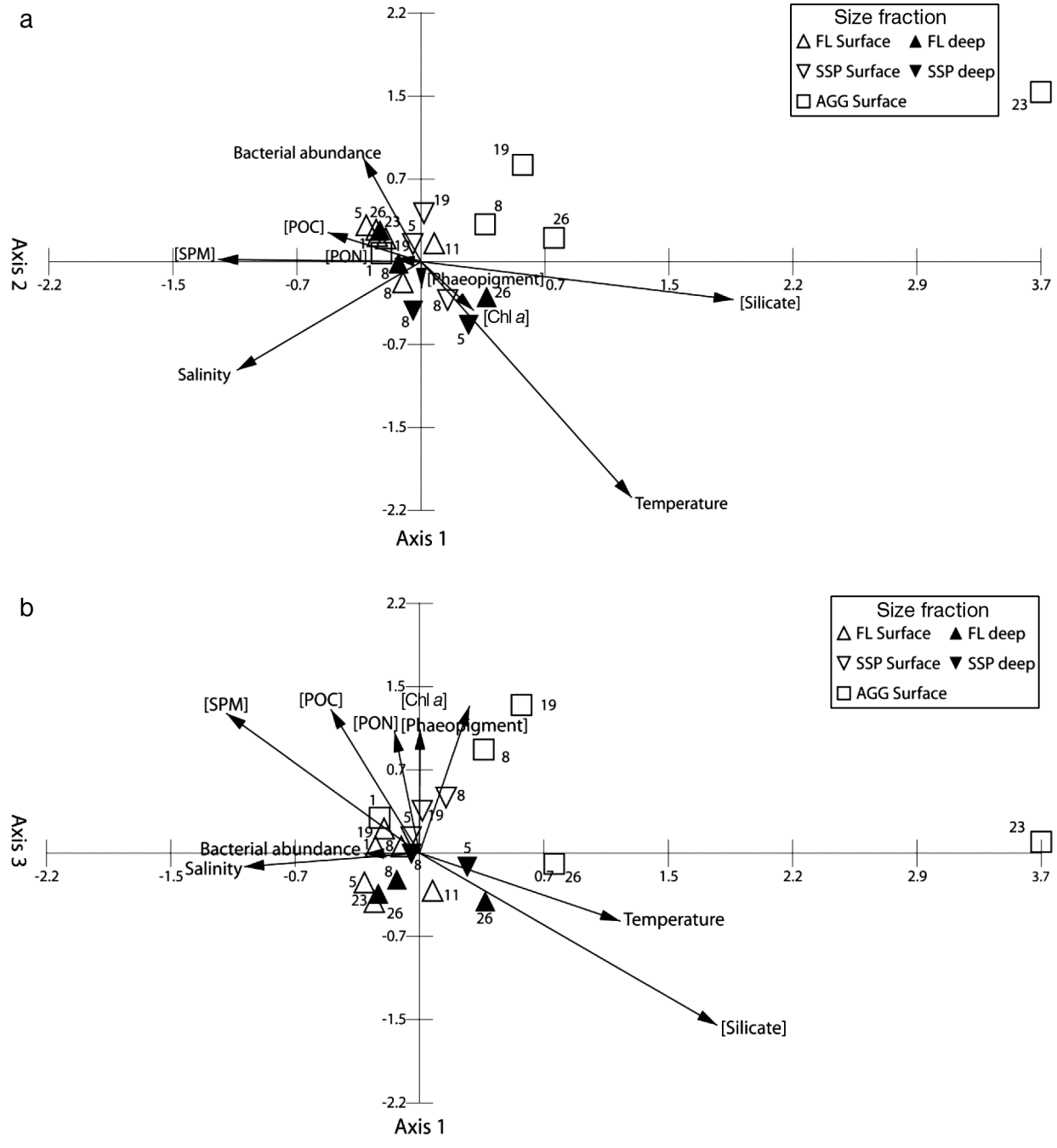

Fig. 6. Results of canonical correspondence analyses, a direct gradient analysis comparing bacterial community structure, estimated by terminal restriction fragment length polymorphism (T-RFLP), to the indicated environmental data. (a): Axes 1 and 2; (b): Axes 1 and 3. Size fractions are AGG: aggregate; FL: free living; or SSP: small suspended particle. POC: particulate organic carbon; PON: particulate organic nitrogen; SPM: suspended particulate matter. Square brackets indicate concentration

environment correlations were high (0.839 to 0.949). For Axes 1 and 3, the strongest correlate was concentration of dissolved silicate (riverine input), followed by temperature for Axis 1. For Axis 2, temperature was strongest, followed by salinity. Measures of particulate matter (chl *a*, POC, and SPM) also helped define Axis 3. FL and SSP bacterial communities tended to group near the origins of the CCA biplots (Fig. 6), reflecting no particular influence by the environmental factors considered, while AGG communities tended to spread along Axis 1 (Fig. 6) in the region of the biplot associated with less than average salinity.

In the CCA comparing archaeal community structure and environmental factors (Fig. 7), most of the variation in the T-RFLP data was again explained by the first 3 axes (22.9, 18.4, and 16.3%) for which spe-

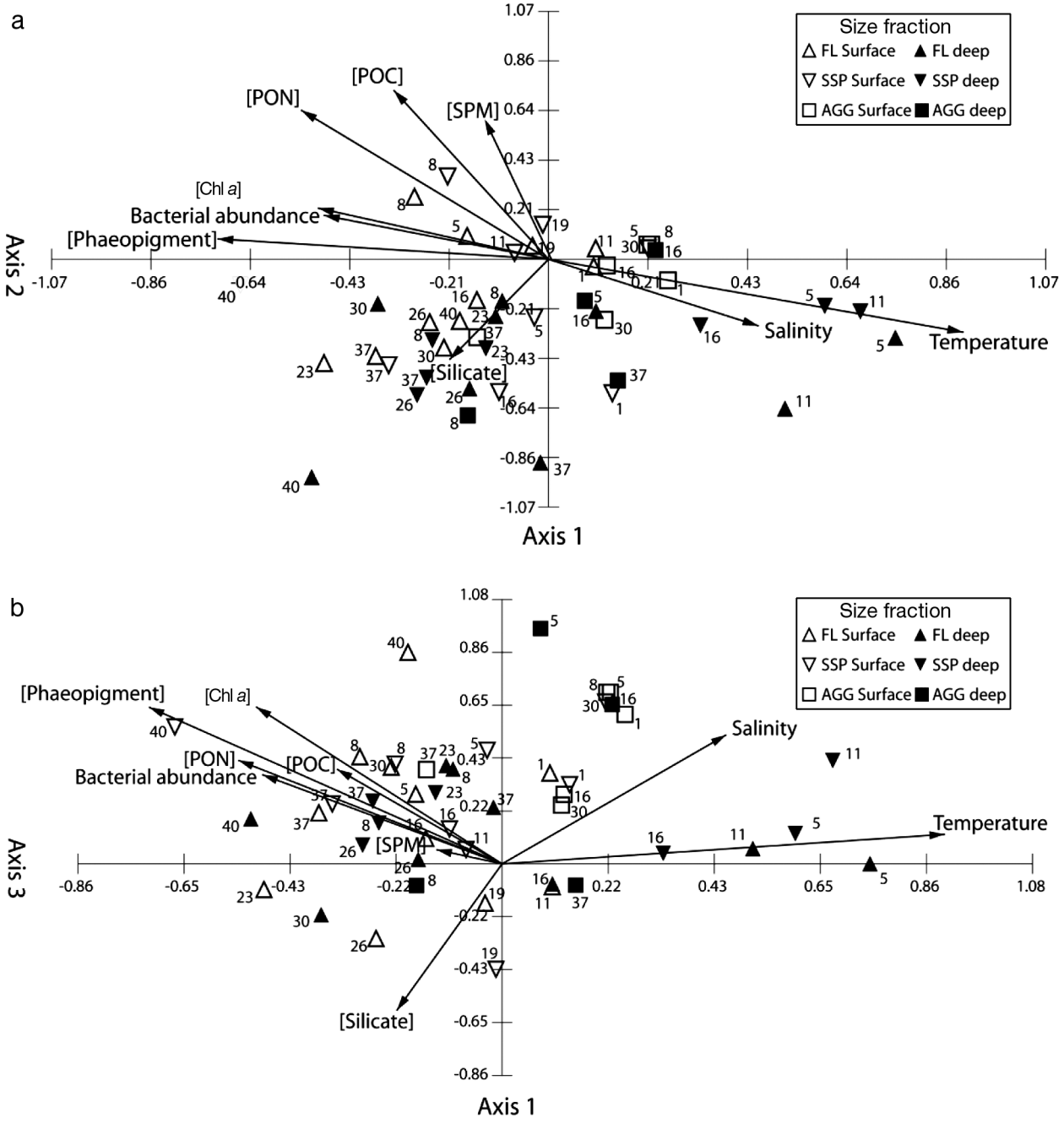

Fig. 7. Results of canonical correspondence analyses, a direct gradient analysis comparing archaeal community structure, estimated by terminal restriction fragment length polymorphism (T-RFLP), to the indicated environmental data. (a): Axes 1 and 2; (b): Axes 1 and 3. Size fractions are AGG: aggregate; FL: free living; or SSP: small suspended particle. POC: particulate organic carbon; PON: particulate organic nitrogen; SPM: suspended particulate matter. Square brackets indicate concentration

cies-environment correlations were also high (0.765 to 0.851). The strongest correlate for Axis 1 was temperature, followed by phaeopigment concentration. General particle loading (POC, PON, and SPM) defined Axis 2, while pigment concentrations, followed by silicate concentration and salinity, defined Axis 3. In contrast to the bacterial CCA, FL and SSP archaeal samples were more dispersed than their AGG counterparts on the biplots (but note reduced axis scales, Fig. 7), with no unifying factor of influence. AGG archaeal samples did not group away from the smaller size fractions, but most deep archaeal samples tended to spread along Axis 1 (Fig. 7), defined most strongly by temperature and phaeopigment concentration.

DISCUSSION

The shelf region of the Laptev Sea operates as a large estuary or mixing zone for particles delivered by the Lena River (Saliot et al. 1996) which resuspend repeatedly on the shelf (Wegner et al. 2005). At the time of our off-shelf sampling, the process of sea-ice rafting (Eicken et al. 1997) may have played a role in particle delivery to a few of the offshore stations (Fig. 1). Coupled with inshore data (Saliot et al. 1996), our characterizations of Laptev Sea waters indicate a river-to-sea gradient in particulate matter, from highest concentrations of SPM and POC in the Lena River (2 to 30 mg l^{-1} and 140 to 950 µg l^{-1}, respectively) to lower levels offshore (6 to 8 mg SPM l^{-1} and 10 to 96 µg POC l^{-1}). A riverine source of particulate matter, even in September (after the river's spring freshet), is consistent with the fresher salinities detected at our eastern and alongshore central stations in the direction of Lena River outflow (Mueller-Lupp et al. 2000, Wegner et al. 2005). It is also consistent with the observed inverse relationship between salinity and dissolved silicate concentration, a proxy for riverine input (the average silicate concentration in the Lena River, 60 µM, is ~10 times that in the Laptev Sea; Kattner et al. 1999) and with isotopic analyses of POM, indicating that ~50% of the material offshore was terrestrial in origin (J. K. Cochran pers. comm.).

During this expedition, the Laptev Sea was post-bloom and widely oligotrophic, as indicated by the low chl *a* and macronutrient concentrations, generally equivalent amounts of chl *a* and phaeopigments, and small fraction of POM represented by pigments (Table 3). Bacterial abundances (range of 1.33×10^5 to 8.19×10^5 cells ml^{-1}) were lower than in the Lena River (6×10^5 to 85×10^5 cells ml^{-1}, Saliot et al. 1996), but overlapped with those reported for nearshore Laptev Sea waters (1.8×10^5 to 20×10^5 cells ml^{-1}, Saliot et al. 1996) and sites in the Western Arctic, including the Chukchi Sea (0.8×10^5 to 8.7×10^5 cells ml^{-1}, Hodges et al. 2005) and the river-impacted Mackenzie Shelf (1.9×10^5 to 18.1×10^5 cells ml^{-1}, Garneau et al. 2006). The decrease in bacterial abundance we observed with depth in the water column was consistent with our stations being offshore and thus beyond the intensive shelf-sediment resuspension zone.

An ideal study of particle-associated bacteria in the Laptev Sea might be undertaken during the spring freshet or bloom season or in an area of intensive sediment resuspension, when levels of particulate matter and bacterial abundance would be higher than those we encountered at the end of the productive season. In spite of the more limited range of conditions we had the opportunity to sample, strong distinctions were observed between microbial communities associated with large aggregates and those communities present in the smaller size fractions. Differently structured and less rich communities on aggregates imply selective environmental forces at work and biogeochemical roles for these microbial communities that may differ from their less-bound counterparts.

Attempts to identify influential environmental forces from our data sets were successful in that the composition of aggregate-associated Bacteria was partially explained by proxies for riverine input (higher dissolved silicate concentrations and fresher salinities; Fig. 6). This result suggests that the riverine influence on pelagic bacterial diversity detected in whole water samples on the Mackenzie Shelf (Garneau et al. 2006) may be attributable to the presence of river-derived aggregates. Our results were less clear for AGG Archaea (even with twice as many amplified samples), but many of these communities appeared linked to marine conditions of higher salinities and warmer temperatures. In the Laptev Sea, warmer marine waters lie at >200 m depths due to incursion of Atlantic water (Dmitrenko et al. 2008).

When all samples (all particle size fractions) were considered collectively by CCA, the one environmental factor observed to influence both bacterial and archaeal community structure was temperature. The cold temperatures of Arctic waters are already understood to constrain microbial activity (Pomeroy & Wiebe 2001), but our result is notable because the evaluated microbial feature was community richness, not activity. Changes in richness, however, can imply microbial succession or dynamics (growth/mortality). In the case of AGG samples, microbial community changes may have occurred during sinking (temperature and depth were highly correlated). Although observed differences in archaeal community structure between surface and deeper water pairs of AGG samples are consistent with this possibility, advection is an equally plausible explanation. Distinctions among microbial

communities involving non-sinking size fractions (SSP and FL) are more likely influenced by temperature than advection.

Our 5 clone libraries, though small in size and generated primarily to assist T-RFLP analyses, are among the first clone libraries available for particle-associated microbes in the Arctic (see Galand et al. 2006 for mention of a particle-associated archaeal clone library from the Mackenzie Shelf). The bacterial libraries fit expectation with regards to composition and diversity. All of them were dominated by members of the *Gammaproteobacteria*, many of which are often found associated with surfaces in the ocean, including sea ice (e.g. species of *Colwellia* and *Marinobacter*, Brinkmeyer et al. 2003). The next most prevalent group, the *Cytophaga-Flavobacteria*, are found enriched in detritus and marine or lake snow (DeLong et al. 1993, Crump et al. 1999, Kirchman 2002, Lemarchand et al. 2006) where they are considered to be particularly important for their production of extracellular enzymes and degradative capabilities (Kirchman 2002). Even *Alphaproteobacteria*, particularly of the *Roseobacter* clade (as detected here), are important colonizers of marine snow (Wagner-Döbler & Biebl 2006).

Further evaluation of bacterial community distinctions using T-RFLP clearly showed that AGG communities differed in both structure and richness from SSP and FL Bacteria. Although studies of temperate marine waters have revealed 2-way distinctions between FL communities and those associated either with particles captured on a 3 µm filter (Crump et al. 1999) or with very large (>400 um) aggregates (DeLong et al. 1993, Rath et al. 1998), our 3-tiered approach to size fractionation allowed recognition of the greater similarity between FL and SSP bacterial communities than between FL and AGG communities. This result implies greater exchange between communities experiencing long residence times in the water column (SSP and FL) relative to aggregates destined to sink to the seafloor (Lee et al. 2004) and possibly resuspend and advect offshore in nepheloid layers (Wells & Deming 2003, Forest et al. 2007).

Regarding Archaea, the overwhelming dominance of MG I Crenarchaeota and thus the limited diversity detected in both of our archaeal libraries (FL and SSP, possibly due to choice of primer sets) was nevertheless consistent with the previously observed trend for MG I Crenarchaeota to increase in abundance offshore and with depth in other waters (Massana et al. 2000, Kirchman et al. 2007). The contents of our archaeal libraries were also consistent with our sampling region falling between river outflow and the central Arctic Ocean: our 2 MG II clones were most closely related to MG II-b clones found inshore on the Mackenzie Shelf (DQ146753, DQ146760, and EF014591; Galand et al. 2006) while all of our MG I clones were closely related to the 1-α cluster described from the central Arctic (Bano et al. 2004).

Both our cloning and T-RFLP approaches to evaluating archaeal communities, the latter revealing greater richness than the former, provided new insight on particle association for this domain. The literature debate on a riverine versus marine source was not resolved (Wells & Deming 2003, Galand et al. 2006, Wells et al. 2006), but the aggregate environment emerged as selective for distinctive archaeal community structures of limited richness, relative to FL counterparts. The same arguments for the importance of particle residence time in structuring bacterial communities also pertain to Archaea, with longer residence times in the water column (for SSP and FL communities) translating to greater archaeal richness. That more specific archaeal communities associate with sinking (or advecting) aggregates merits further study, both in terms of biogeochemical roles in attenuating carbon fluxes via possible heterotrophy in Arctic waters (Kirchman et al. 2007) and possible benefits from chemical gradients created within the aggregates themselves (Alldredge & Cohen 1987, Simon et al. 2002). The absence of overlap in 2D space for pairs of surface-water and deep aggregate-associated archaeal communities (Fig. 5) and the tendency of deep archaeal communities to spread along the CCA axis defined by temperature and phaeopigment concentration (Axis 1, Fig. 7) point to testable hypotheses on microbial selection during aggregate sinking.

In summary, the results of our 3-tiered size-fractionation approach demonstrated both by clone libraries and T-RFLP analyses that strong differences in bacterial and archaeal communities exist between large aggregates (>60 um) and smaller suspended particles in the cold waters of the Laptev Sea. More exchange is evident between free-living communities and those associated with smaller particles than between either of these suspended communities and those associated with large sinking aggregates. Although some of the variation in bacterial community structure could be attributed to riverine influence, other environmental factors measured on different scales than we attempted are needed to better define the drivers of particle-associated community structure for both Bacteria and Archaea in this region. The occurrence of distinguishable aggregate-associated microbial communities throughout the study area and hints of changes with depth, despite seasonally diminished inputs from the Lena River and marine primary production, suggest their importance in the attenuation of vertical and off-shelf fluxes of POM.

Acknowledgements. This research was supported by an NSF fellowship to C.T.E.K. and by NSF-OPP award ARC-0520297 to J.W.D. We thank I. Dmitrenko for the invitation to join NABOS 2005 as part of the International Summer School conducted on board and for access to CTD data, M. Nitishinsky for access to nutrient data, S. D. Carpenter for analyzing POC, PON, and chl *a* samples and for technical assistance and support, R. E. Collins for helpful discussion, and J. K. Cochran for collaboration in the field and regarding data analyses. We also thank the anonymous reviewers whose constructive comments helped us to improve an earlier version of this manuscript.

LITERATURE CITED

Alldredge AL, Cohen Y (1987) Can microscale chemical patches persist in the sea? Microelectrode study of marine snow, fecal pellets. Science 235:689–691

Amann RI, Ludwig W, Schleifer KH (1995) Phylogenetic identification and in situ detection of individual microbial cells without cultivation. Microbiol Mol Biol Rev 59:143–169

Amiel D, Cochran JK, Hirschberg DJ (2002) $^{234}Th/^{238}U$ disequilibrium as an indicator of the seasonal export flux of particulate organic carbon in the North Water. Deep Sea Res Part II 49:5191–5209

Ashelford KE, Chuzhanova NA, Fry JC, Jones AJ, Weightman AJ (2006) New screening software shows that most recent large 16S rRNA gene clone libraries contain chimeras. Appl Environ Microbiol 72:5734–5741

Bano N, Hollibaugh JT (2002) Phylogenetic composition of bacterioplankton assemblages from the Arctic Ocean. Appl Environ Microbiol 68:505–518

Bano N, Ruffin S, Ransom B, Hollibaugh JT (2004) Phylogenetic composition of Arctic Ocean archaeal assemblages and comparison with Antarctic assemblages. Appl Environ Microbiol 70:781–789

Bates NR, Hansell DA, Moran SB, Codispoti LA (2005) Seasonal and spatial distribution of particulate organic matter (POM) in the Chukchi and Beaufort Seas. Deep Sea Res Part II 52:3324–3343

Boetius A, Damm E (1998) Benthic oxygen uptake, hydrolytic potentials and microbial biomass at the Arctic continental slope. Deep Sea Res Part I 45:239–275

Brinkmeyer R, Knittel K, Jurgens J, Weyland H, Amann R, Helmke E (2003) Diversity and structure of bacterial communities in Arctic versus Antarctic pack ice. Appl Environ Microbiol 69:6610–6619

Buesseler KO (1998) The de-coupling of production and particulate export in the surface ocean. Global Biogeochem Cycles 12:297–310

Carroll ML, Carroll J (2003) The Arctic seas. In: Black KD, Shimmield GB (eds) Biogeochemistry of marine systems. Blackwell Academic Press, Oxford p 127–147

Cho BC, Azam F (1988) Major role of bacteria in biogeochemical fluxes in the ocean's interior. Nature 332:441–443

Cochran JK, Barnes C, Achman D, Hirschberg DJ (1995) $^{234}Th/^{238}U$ disequilibrium as an indicator of scavenging rates and particulate organic carbon fluxes in the Northeast Water Polynya, Greenland. J Geophys Res 100(C3): 4399–4410 doi:10.1029/945C01954

Collins RE, Rocap G (2007) REPK: an analytical web server to select restriction endonucleases for terminal restriction fragment length polymorphism analysis. Nucleic Acids Res 35:W58–W62

Collins RE, Carpenter SD, Deming JW (2008) Spatial heterogeneity and temporal dynamics of particles, bacteria, and pEPS in Arctic winter sea ice. J Mar Syst 74:902–917

Crump BC, Armbrust EV, Baross JA (1999) Phylogenetic analysis of particle-attached and free-living bacterial communities in the Columbia River, its estuary and the adjacent coastal ocean. Appl Environ Microbiol 65:3192–3204

Crump BC, Bahr M, Kling GW, Hobbie JE (2003) Bacterioplankton community shifts in an arctic lake correlate with seasonal changes in organic matter source. Appl Environ Microbiol 69:2253–2268

Dang H, Lovell CR (2002) Seasonal dynamics of particle-associated and free-living marine *Proteobacteria* in a salt marsh tidal creek as determined using fluorescence *in situ* hybridization. Environ Microbiol 4:287–295

DeLong EF (1992) Archaea in coastal marine environments. Proc Natl Acad Sci USA 89:5685–5689

DeLong EF, Franks DG, Alldredge AL (1993) Phylogenetic diversity of aggregate-attached vs. free-living marine bacterial assemblages. Limnol Oceanogr 38:924–934

DeSantis TZ, Hugenholtz P, Larsen N, Rojas M and others (2006) Greengenes, a chimera-checked 16S rRNA gene database and workbench compatible with ARB. Appl Environ Microbiol 72:5069–5072

Dmitrenko IA, Polyakov IV, Kirillov SA, Timokhov LA and others (2008) Towards a warmer Arctic Ocean: spreading of the early 21st century Atlantic Water warm anomaly along the Eurasian Basin margins. J Geophys Res Oceans 113:C05023 doi:10.1029/2007JC004158

Eicken H, Reimnitz E, Alexandrov V, Martin T, Kassens H, Viehoff T (1997) Sea-ice processes in the Laptev Sea and their importance for sediment export. Cont Shelf Res 17: 205–233

Fandino LB, Riemann L, Steward GF, Long RA, Azam F (2001) Variations in bacterial community structure during a dinoflagellate bloom analyzed by DGGE and 16S rDNA sequencing. Aquat Microb Ecol 23:119–130

Forest A, Sampei M, Hattori H, Makabe R and others (2007) Particulate organic carbon fluxes on the slope of the Mackenzie Shelf (Beaufort Sea): physical and biological forcing of shelf-basin exchanges. J Mar Syst 68:39–54

Galand PE, Fritze H, Yrjälä K (2003) Microsite-dependent changes in methanogenic populations in a boreal oligotrophic fen. Environ Microbiol 5:1133–1143

Galand PE, Lovejoy C, Vincent WF (2006) Remarkably diverse and contrasting archaeal communities in a large arctic river and the coastal Arctic Ocean. Aquat Microb Ecol 44:115–126

Garneau ME, Vincent WF, Alonso-Sáez L, Gratton Y, Lovejoy C (2006) Prokaryotic community structure and heterotrophic production in a river-influenced coastal arctic ecosystem. Aquat Microb Ecol 42:27–40

Großkopf R, Janssen PH, Liesack W (1998) Diversity and structure of the methanogenic community in anoxic rice paddy soil microcosms as examined by cultivation and direct 16S rRNA gene sequence retrieval. Appl Environ Microbiol 64:960–969

Hammer Ø, Harper DAP, Ryan PD (2008) Paleontological statistics version 1.79, data analysis package. http://folk.uio.no/ohammer/past/

Hodges LR, Bano N, Hollibaugh JT, Yager PL (2005) Illustrating the importance of particulate organic matter to pelagic microbial abundance and community structure — an Arctic case study. Aquat Microb Ecol 40:217–277

Holland MM, Finnis J, Barrett AP, Serreze MC (2007) Projected changes in Arctic Ocean freshwater budgets. J Geophys Res Biogeosci 112:G04S55 doi:10.1016/S0967-0645(02)00186-8

Huston AL, Deming JW (2002) Relationships between microbial extracellular enzymatic activity and suspended and

sinking particulate organic matter: seasonal transformations in the North Water. Deep Sea Res Part II 49: 5211–5225

Johnson W, Lewitus AJ, Fletcher M (2006) Linking bacterioplankton community structures to environmental state variables and phytoplankton assemblages in two South Carolina salt marsh estuaries. Aquat Microb Ecol 45: 129–145

Karner M, Herndl GJ (1992) Extracellular enzymatic activity and secondary production in free-living and marine-snow-associated bacteria. Mar Biol 113:341–347

Kattner G, Lobbes JM, Fitznar HP, Engbrodt R, Nothig EM, Lara RJ (1999) Tracing dissolved organic substances and nutrients from the Lena River through Laptev Sea (Arctic). Mar Chem 65(1–2):25–39

Kirchman DL (2002) MiniReview: the ecology of *Cytophaga-Flavobacteria* in aquatic environments. FEMS Microbiol Ecol 39:91–100

Kirchman DL, Elifantz H, Dittel AI, Malmstrom RR, Cottrell MT (2007) Standing stocks and activity of Archaea and bacteria in the western Arctic Ocean. Limnol Oceanogr 52:495–507

Lane DJ (1991) 16S/23S rRNA sequencing. In: Stackebrandt E, Goodfellow M (eds) Nucleic acid techniques in bacterial systematics. John Wiley & Sons, New York, p 115–175

Lee C, Wakeham S, Arnosti C (2004) Particulate organic matter in the sea: the composition conundrum. Ambio 33: 566–575

Lemarchand C, Jardillier L, Carrias JF, Richardot M, Debroas D, Sime-Ngando T, Amblard C (2006) Community composition and activity of prokaryotes associated with detrital particles in two contrasting lake ecosystems. FEMS Microbiol Ecol 57:442–451

Massana R, Murray AE, Preston CM, DeLong EF (1997) Vertical distribution and phylogenetic characterization of marine planktonic *Archaea* in the Santa Barbara Channel. Appl Environ Microbiol 63:50–56

Massana R, DeLong E, Pedrós-Alió C (2000) A few cosmopolitan phylotypes dominate planktonic archaeal assemblages in widely different oceanic provinces. Appl Environ Microbiol 66:1777–1787

Moeseneder MM, Arrieta JM, Muyzer G, Winter C, Herndl GJ (1999) Optimization of terminal-restriction fragment length polymorphism analysis for complex marine bacterioplankton communities and comparison with denaturing gradient gel electrophoresis. Appl Environ Microbiol 65:3518–3525

Moyer CL, Tiedje JM, Dobbs FC, Karl DM (1998) Diversity of deep-sea hydrothermal vent Archaea from Loihi Seamount, Hawaii. Deep Sea Res Part II 45(1–3):303–317

Mueller-Lupp T, Bauch HA, Erlenkeuser H, Hefter J, Kassens H, Theide J (2000) Changes in the deposition of terrestrial organic matter on the Laptev Sea shelf during the Holocene: evidence from stable carbon isotopes. Int J Earth Sci 89:563–568

Parsons TR, Maita Y, Lalli CM (1984) A manual of chemical and biological methods for seawater analysis. Pergamon Press, Oxford

Pomeroy LR, Wiebe WJ (2001) Temperature and substrates as interactive limiting factors for marine heterotrophic bacteria. Aquat Microb Ecol 23:187–204

Rath J, Wu KY, Herndl GJ, DeLong EF (1998) High phylogenetic diversity in a marine-snow-associated bacterial assemblage. Aquat Microb Ecol 14:261–269

Saliot A, Cauwet G, Cahet G, Mazaudier D, Daumas R (1996) Microbial activities in the Lena River delta and Laptev Sea. Mar Chem 53:247–254

Schloss PD, Handelsman J (2005) Introducing DOTUR, a computer program for defining operational taxonomic units and estimating species richness. Appl Environ Microbiol 71:1501–1506

Schmidt JL, Deming JW, Jumars PA, Keil RG (1998) Constancy of bacterial abundance in surficial marine sediments. Limnol Oceanogr 43:976–982

Selje N, Simon M (2003) Composition and dynamics of particle-associated and free-living bacterial communities in the Weser estuary, Germany. Aquat Microb Ecol 30:221–237

Serreze MC, Holland MM, Stroeve J (2007) Perspectives on the Arctic's shrinking sea-ice cover. Science 315: 1533–1536

Simon M, Grossart HP, Schweitzer B, Ploug H (2002) Microbial ecology of organic aggregates in aquatic ecosystems. Aquat Microb Ecol 28:175–211

Suzuki MT, Giovannoni SJ (1996) Bias caused by template annealing in the amplification of mixtures of 16S rRNA genes by PCR. Appl Environ Microbiol 62:625–630

Van Mooy BAS, Devol AH, Keil RG (2004a) Quantifying ^{3}H-thymidine incorporation rates by a phylogenetically defined group of marine planktonic bacteria (Bacteriodetes phylum). Environ Microbiol 6:1061–1069

Van Mooy BAS, Devol AH, Keil RG (2004b) Relationships between bacterial community structure, light, and carbon cycling in the eastern subarctic North Pacific. Limnol Oceanogr 48:1056–1062

Wagner-Döbler I, Biebl H (2006) Environmental biology of the marine *Roseobacter* lineage. Annu Rev Microbiol 60: 255–280

Wegner C, Holemann JA, Dmitrenko I, Kirillov S, Kassens H (2005) Seasonal variations in Arctic sediment dynamics – evidence from 1-year records in the Laptev Sea (Siberian Arctic). Global Planet Change 48:126–140

Wells LE, Deming JW (2003) Abundance of bacteria, the *Cytophaga-Flavobacterium* cluster and Archaea in cold oligotrophic waters and nepheloid layers of the Northwest Passage, Canadian Archipelago. Aquat Microb Ecol 31: 19–31

Wells LE, Cordray M, Bowerman S, Miller LA, Vincent WF, Deming JW (2006) Archaea in particle-rich waters of the Beaufort Shelf and Franklin Bay, Canadian Arctic: clues to an allochthonous origin? Limnol Oceanogr 51:47–59

Appendix 1. Laptev Sea environmental variables

Table A1. Environmental variables measured at each station (and used in Fig. A1). Values for particulate factors are average concentrations (n = 2). nd: no data; SPM: suspended particulate matter; POC: particulate organic carbon; PON: particulate organic nitrogen; Phaeo: phaeopigments

Stn		Sample			Particulate factor					
Number	Depth (m)	Depth (m)	Temp. (°C)	Salinity	SPM (mg l^{-1})	POC (µg l^{-1})	PON (µg l^{-1})	Chl *a* (µg l^{-1})	Phaeo (µg l^{-1})	Bacteria (× 10^5 cells ml^{-1})
Western Laptev										
1	1100	25	–1.63	33.3	nd	59.8	9.1	0.18	0.19	6.4
5	1600	25	–1.62	33.2	6.6	95.5	12.7	0.07	0.16	5.9
		150	1.49	34.8	6.8	28.9	4.3	0.01	0.06	1.5
8	270	25	–1.36	34.1	7.3	87.3	13.1	0.21	0.19	3.3
		100	–1.34	34.6	6.6	43.1	6.5	0.03	0.06	1.6
11	1650	25	–1.62	33.1	nd	51.0	8.2	nd	nd	6.6
		150	1.26	34.8	nd	20.9	3.6	nd	nd	1.9
Central Laptev										
16	2600	25	–1.53	30.5	7.3	48.3	5.8	0.07	0.07	6.3
		100	–1.37	34.2	6.7	35.7	6.7	0.01	0.02	1.3
19	3100	25	–1.61	30.2	7.0	36.0	5.0	0.01	0.04	1.8
37	2200	25	–1.31	32.0	5.9	46.6	9.1	0.17	0.18	8.2
		100	–1.07	34.3	6.6	10.3	3.6	0.01	0.01	1.8
40	102	25	–1.11	33.3	7.2	40.5	8.3	0.68	0.53	6.2
		60	–1.09	33.9	7.1	43.7	5.9	0.05	0.23	2.6
Eastern Laptev										
23	1600	25	–1.52	31.4	6.0	53.0	8.2	0.08	0.09	3.8
		100	–1.41	34.1	7.1	30.1	5.2	0.01	0.03	1.5
26	1330	25	–0.54	28.6	6.6	25.3	7.2	0.11	0.11	3.4
		100	–1.46	34.0	6.4	14.3	4.0	0.01	0.03	2.0
30	90	25	–0.19	31.8	6.3	34.5	6.1	0.08	0.09	4.6
		75	–1.41	33.7	7.7	36.4	7.1	0.06	0.15	3.8

Appendix 2. Principal component analysis of Laptev Sea environmental data

To assess how stations grouped together by their physical-chemical characteristics, a principal component analysis (PCA) was conducted on environmental data collected in the Laptev Sea (Fig. A1). The first and second principal axes of this PCA explained 37 and 23%, respectively, of the variance between samples. Visual inspection of the PCA biplot revealed that all surface water samples group separately from all deeper samples. A follow-up ANOVA confirmed that the first principal axis varies highly significantly with depth ($p << 0.001$).

Further separation in the data was observed along the first principal axis, where eigenvectors for the physical-chemical factors of temperature, salinity, and inorganic nutrients point to the right of the origin (where all but one deeper sample locate) and those for the particulate variables of pigment, bacterial, and particulate organic matter (POM) concentrations point left (where all but one surface sample locate). The second axis had significant positive eigenvector loadings for the pigment concentrations and a negative loading for silicate concentration, suggesting a gradient between primary production and silicate input. All of the surface samples from stations characterized as river-impacted by their relatively fresh salinities (Stns 16, 19, 23, 26, and 30) grouped below the origin of the biplot, where the eigenvector for silicate also plotted. In contrast, all of the surface samples with more marine salinities (from Stns 1, 5, 8, 11, 37, and 40) grouped in the first quadrant of the biplot (upper left), along with the eigenvectors for particulate parameters. Overall, this PCA yielded a geographic pattern consistent with more recent primary production in (marine) western and alongshore stations than at (river-influenced) eastern and offshore locations

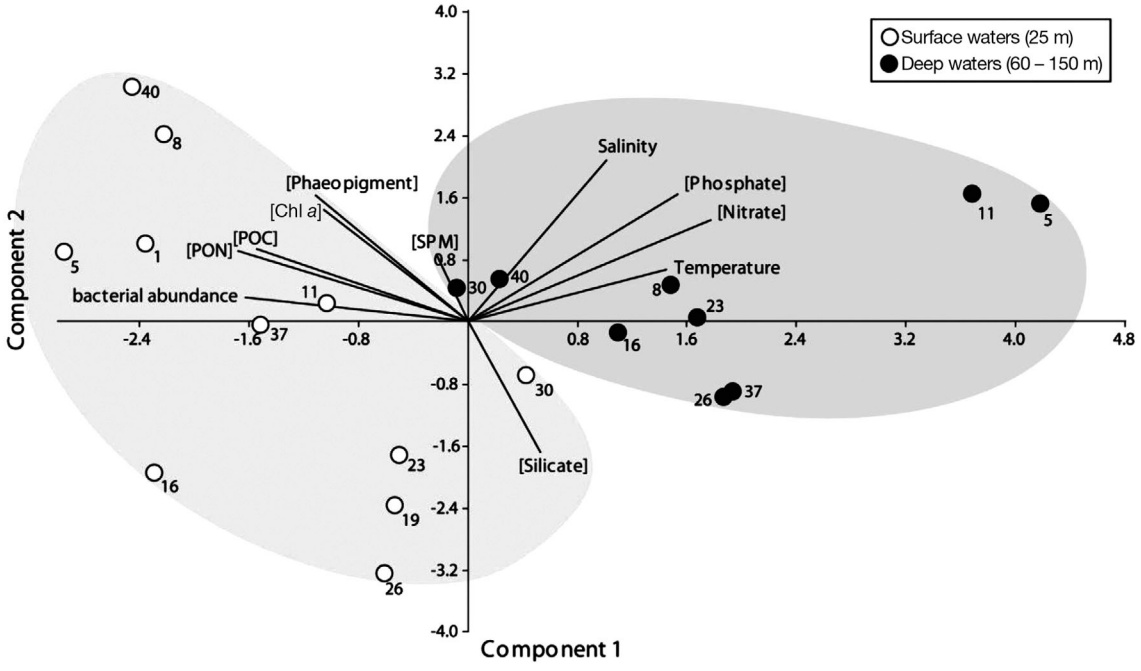

Fig. A1. Principal component analyses of the indicated environmental variables. Numbers next to symbols indicate station number (see Fig. 1). Shaded areas indicate the separate groupings of shallow and deep samples. POC: particulate organic carbon; PON: particulate organic nitrogen; SPM: suspended particulate matter. Square brackets indicate concentration

Editorial responsibility: Craig Carlson, Santa Barbara, California, USA

Submitted: March 31, 2008; Accepted: May 04, 2009
Proofs received from author(s): July 10, 2009